Published in final edited form as:
Ann N Y Acad Sci. 2010 March ; 1192(1): 84–94. doi:10.1111/j.1749-6632.2009.05210.x.

Effects of anti-resorptive agents on osteomyelitis: Novel insights on osteonecrosis of the jaw (ONJ) pathogenesis

Dan Li[1,*], **Kirill Gromov**[1,2,*], **Steven T. Proulx**[1], **Chao Xie**[1], **Jie Li**[1], **Daniel P. Crane**[1], **Kjeld Søballe**[2], **Regis J. O'Keefe**[1], **Hani A. Awad**[1,3], **Lianping Xing**[1], and **Edward M. Schwarz**[1,4]

[1] The Center for Musculoskeletal Research, University of Rochester, Rochester, New York

[2] The Department of Orthopedics, Aarhus University Hospital, Aarhus, Denmark

[3] Department of Biomedical Engineering, University of Rochester, Rochester, New York

Abstract

The effects of anti-resorptive agents (i.e. alendronate (Aln), osteoprotegerin (OPG)) on bone infection are unknown. Thus, their effects on implant-associated osteomyelitis (OM) were investigated in mice using PBS (placebo), gentamycin and etanercept (TNFR:Fc) controls. None of the drugs affected humoral immunity, angiogenesis, or chronic infection. However, the significant ($p<0.05$ vs. PBS) inhibition of cortical osteolysis and decreased draining lymph node size in Aln and OPG treated mice was associated with a significant ($p<0.05$) increase in the incidence of high-grade infections during the establishment of OM. In contrast, the high-grade infections in TNFR:Fc treated mice were associated with immunosuppression, as evidenced by the absence of granulomas and presence of $Gram^+$ biofilm in the bone marrow. Collectively, these findings indicate that while anti-resorptive agents do not exacerbate chronic OM, they can increase the bacterial load during early infection by decreasing lymphatic drainage and preventing the removal of necrotic bone that harbors the bacteria.

INTRODUCTION

Although the incidence of orthopaedic bone infection, known as osteomyelitis (OM), for joint prostheses and fracture-fixation devices have remained at 0.3–11% and 5–15% respectively over the last decade [1,2], the emergence of methicillin-resistant *Staphylococcus aureus* (MRSA) has dramatically impacted clinical management [3,4]. Since OM induces osteolysis around the implant, which can lead to fractures and complicate revision surgery, orthopedists have anecdotally used anti-resorptive bisphosphonates in these patients to preserve bone stock without knowledge of their effects on chronic infection [5,6].

Another clinical condition that is associated with OM and bisphosphonate use is osteonecrosis of the jaw (ONJ) epidemic [7,8], which primarily affects cancer patients on immunosuppressive chemotherapy that also receive intravenous pamidronate or zoledronate for hypercalcaemia, and undergo unrelated oral surgery [9,10]. However, ONJ has also been reported in healthy women taking oral alendronate for postmenopausal osteoporosis [9,10], raising serious concerns for the tens of millions of people taking these anti-resorptive agents. Although the etiology of ONJ remains unknown, careful reviews of all the available clinical and basic science data have derived two leading theories to explain this painful condition [11–13]. The first is inhibition of

[4]To whom correspondence should be addressed: Dr. Edward M. Schwarz, The Center for Musculoskeletal Research, University of Rochester Medical Center, 601 Elmwood Avenue, Box 665, Rochester, NY 14642, Phone 585-275-3063, FAX 585-756-4727, Edward_Schwarz@URMC.Rochester.edu.
*These authors contributed equally to this work.

angiogenesis, which is largely derived from the precedent of steroid-induced avascular necrosis of the hip, and new studies that have demonstrated bisphosphonate-inhibition of capillary tube formation, vessel sprouting and circulating endothelial cells [14–16]. The other is the osteoclast-inhibiting effect of anti-resorptive agents that lead to a cessation of bone remodeling and mineral:matrix turnover [10]. This renders the fatigued bone susceptible to involution of blood vessels, necrosis and infection. The impact of infection in ONJ is further highlighted by the finding that essentially all cases have histopathological evidence of OM [17,18], however, a cause and effect relationship has yet to be established.

To better understand the effects of bisphosphonates on OM, and shed light on potential mechanisms of ONJ, we investigated the interaction of anti-resorptive agents in an established murine trans-tibial infected pin model that emulates the biology of infected orthopaedic and periodontal implants [19]. This model takes advantage of a gentamycin sensitive, *luxA-E* transformed stain of *S. aureus* (Xen29) [20], whose metabolic activity and bacterial load can be quantified *in vivo* using longitudinal bioluminescence imaging (BLI) and *nuc* quantitative real-time PCR (QRT-PCR) respectively [19]. This model also has micro-CT outcome measures of osteolysis and vascularity, serological analyses of the protective IgG2b humoral response that appears by day 11, and traditional histology of osteoclasts and Gram-stained biofilm [19]. Here we investigated two distinct classes of anti-resorptive drugs: the most widely prescribed bisphosphonate alendronate (Aln) [8], which induces osteoclast apoptosis via inhibition of the mevalonate pathway of isoprenoid biosynthesis [21]; and the biologic antagonists osteoprotegerin (OPG) that inhibits osteoclast formation and induces osteoclast apoptosis by blocking receptor activator of nuclear factor kappa B (RANK) signaling pathway [22]. While these studies demonstrated that neither Aln nor OPG could induce or exacerbate chronic OM, likely because they do not affect the protective humoral response nor inhibit angiogenesis in our model, both agents caused an increase in high-grade infections as defined by significant increases in the number of mice with BLI and *nuc* gene levels above maximum placebo levels. This finding coincided with a significant decrease in osteolysis and draining lymph node size, suggesting that anti-resorptive agents decrease efflux of marrow lymph during the establishment of OM. Thus, these effects could lead to a dramatic increase in intraosseous pressure, infarction and bone pain, which are the hallmarks of OM and ONJ.

MATERIALS AND METHODS

Murine OM model and drug treatments

All animal studies were performed under University of Rochester Committee for Animal Resources approved protocols. Pathogenic challenges with *S. aureus* Xen29 were performed as previously described [19]. Drug treatments started on the day of surgery, except for Aln, which started 3 days before surgery. Aln (Calbiochem, San Diego, CA) was given at 10μg/kg i.p. once every 3 days. OPG (R&D Systems, Minneapolis, MN) was given at 200μg i.p. once every 3 days. TNFR:Fc (Amgen, Thousand Oaks, CA) was given at 200μg i.p. once every 3 days. Placebo was given as 200μl PBS i.p. once every 3 days. Gentamycin (Calbiochem, San Diego, CA) was given daily (0.1 mg/kg i.p.).

Radiology, Bioluminescent Imaging, Micro-CT and MRI

Longitudinal osteolysis was assessed radiographically using a Faxitron Cabinet x-ray system (Faxitron, Wheeling, IL, USA) [19]. Bioluminescent imaging (BLI) of mice infected with Xen29 was performed on day 0, 4, 7, 11, 14, 18 post-infection as previously described [19]. Micro-CT and vascular micro-CT was performed as previously described [23,24]. CE-MRI was performed as previously described [25,26].

Histologic evaluation of OM

After micro-CT, the tibial samples were processed for decalcified histology and stained with Orange G/alcian blue (H&E), Gram-stained, or stained for tartrate-resistant acid phosphatase (TRAP) activity as we have described previously [27]. Immunohistochemistry to identify T-cells, B-cells, macrophages and neutrophils was performed as described previously [28], using primary antibodies specific for CD3 (diluted 1:100; Novocastra, Newcastle, UK), CD45R/B220 (diluted 1:300; BD Biosciences Pharmingen, San Jose, CA, USA), F4/80 (diluted 1:80; AbD Serotec, Raleigh, NC, USA), and Neu7/4 (clone# MCA771G, diluted 1:2000, AbD Serotec, Raleigh, NC) respectively. Osteoclasts were quantified as the mean +/− SD number of TRAP + multinucleated cells in the 10x field centered on the pin tract from three contiguous 3 μm sections 500μm apart, as previously described [29].

DNA purification and nuc/β-actin RTQ-PCR

Total DNA was extracted from infected tibiae and analyzed by RTQ-PCR for the *S. aureus*-specific *nuc* gene standardized to mouse *β-actin* as previously described [19].

Statistical analysis

All values are presented as means ± SD. Significant differences between groups in the histology, micro-CT, serology, MRI and PLN weight analyses were determined by ANOVA with Bonferroni correction. A Fisher's exact test was performed to determine significant differences in the incidence of infection and high-grade infection. The correlation between BLI vs. *nuc* was estimated using Pearson's correlation coefficient and tested for significance using a two-sided *t*-test. In all cases, $p<0.05$ was considered significant.

RESULTS

Anti-resorptive drug effects on osteoclast numbers, necrotic bone and biofilm in chronic OM

In order to assess the effects of anti-resorptive agents on the establishment of implant-associated OM, we investigated five experimental groups in the Xen29-infected trans-tibial pin model [19]: Group 1 received effective gentamycin prophylaxis that prevents infection (Gent), Group 2 received placebo (PBS), Group 3 received OPG, Group 4 received Aln, and Group 5 received the tumor necrosis factor (TNF) antagonist etanercept (TNFR:Fc) as a control that is known to inhibit osteoclasts [30] and exacerbate infections by inhibiting granuloma formation [31]. Upon initial inspection of the x-rays taken on day 18, effects of all three anti-resorptive treatments displayed remarkable large soft-tissue abscesses compared to the Gent and PBS controls (Fig. 1A–E). Histological analyses of these tibiae also confirmed the significant effects of these drugs on the reduction of osteoclasts numbers at the bone-implant interface (Fig. 1F–O). Although TNF blockade also reduced osteoclast numbers to a certain extent, it is noteworthy that the effects of TNFR:Fc on bone histology were significantly different from all of the other groups, indicating a different mechanism of action. Consistent with the osteoclast results, we found that OPG and Aln treated mice had large amounts of unresorbed necrotic cortical bone adjacent to the pin tract (Fig. 1H–I, M–N), which served as a nidus for infection as evidenced by the presence of $Gram^+$ biofilm in parallel sections (Fig. 1R–S). In contrast, the extensive osteolysis in the PBS and TNFR:Fc treated mice appeared to have removed all of the necrotic bone around the pin hole (Fig. 1G, J), and there was no evidence of bacteria at these sites in parallel sections (Fig. 1L, O). However, infection in these animals was evident from $Gram^+$ biofilm within necrotic bone fragments that were likely generated during implantation of the pin (Fig. 1Q, T). As expected from effective prophylaxis, Gent treated mice had no evidence of osteolysis or infection (Fig. 1A,F,K,P).

Anti-resorptive drugs increase the incidence of high-grade infections during the establishment of chronic OM

In order to assess the effects of Aln, OPG and TNFR:Fc on Xen29 metabolism and bacterial load during the establishment of implant-associated OM, we performed longitudinal BLI before, during and after the establishment of protective humoral immunity (Days 7, 11, 18, respectively) in our model [19] (Fig. 2A–C). While these experiments failed to demonstrate any significant differences between the averages of the groups ($p>0.05$), indicating that the drugs cannot exacerbate infection by themselves, we did observe a few mice in the OPG, Aln and TNFR:Fc groups that had remarkably high BLI values, suggestive of "high-grade" infection. To test this we performed Fisher's exact tests comparing the number of uninfected, infected and high-grade infected mice in each group (Fig. 2A–C). These results demonstrated that while Aln and OPG did not increase the incidence of infection at any time they caused a significant increase in the number of mice with high-grade infections early on (Day 7 and 11). Interestingly, the effects of TNFR:Fc were similar with the exception that TNF inhibition caused a 100% infection rate on Day 7.

In order to confirm our observation that anti-resorptive drugs induce high-grade infections during the establishment of OM, we quantified the bacterial load on day 7 and day 18 (Figs. 2D–E). Interestingly, while no differences were observed early on, the OPG, Aln and TNFR:Fc groups all had significantly more high-grade chronic infections on day 18. In order to demonstrate that the high-grade infections determined by BLI and RTQ-PCR were in the same animals, we performed a linear regression analysis of all the day 18 data (Fig. 2F). This significant correlation ($R^2=0.64$, $p<0.05$) validates our findings that anti-resorptive agents can increase the incidence of high-grade OM.

Anti-resorptive drug effects on osteolysis, angiogenesis and immunity during the establishment of chronic OM

In order to better understand the mechanism by which anti-resorptive drugs increase the incidence of high-grade OM, we investigated their effects on bone volume, vasculature and host immune responses during the infection. First, we performed micro-CT analyses on the infected tibiae to assess bone and vasculature around the pin on day 18. While the micro-CT images of the bone corroborated the x-ray and histology findings (Fig. 1), the most striking result was the zone of inhibited reactive bone formation around the infected pins of Aln and OPG treated mice (Fig. 3A). This zone appeared as an almost perfect ring ~2mm in diameter, and is the first formal demonstration that OM-induced osteolysis observed in radiographs is largely due to inhibition of bone formation rather than pure osteoclastic bone resorption. Independent quantification of the osteolytic area in the cortical and reactive bone demonstrated that Aln and OPG completely inhibit cortical resorption, but have no effects on reactive bone formation (Fig. 3B). In contrast, despite its ability to decrease osteoclast numbers and promote high-grade OM, TNFR:Fc did not significantly inhibit cortical osteolysis compared to PBS controls.

Given that avascular necrosis is often associated with OM, we also quantified vascularity in the infected tibiae via 3D vascular micro-CT of lead chromate perfused vessels. These studies failed to detect any significant differences between any of the five groups in terms of vasculature volume, vessel thickness, vessel density, vessel spacing, and degree of anisotropy (data not shown). Thus, none of the drug effects in our model can be explained by changes in angiogenesis.

To test if drug induced immunosuppression of humoral immunity was responsible for the high-grade infections, we examined total Ig levels in sera from the animals over the course of infection. No remarkable serologic differences between groups were observed during the

course of OM (data not shown). These data confirmed the induction of the previously characterized IgG2b response in all of the mice, and demonstrate that none of the drugs inhibited humoral immunity against Xen29. This finding is consistent with the 100% survival rate from a bacterial challenge that would cause lethal sepsis in immunodeficient mice. We also reanalyzed the histology to assess drug effects on granuloma formation (Fig. 4A–H). Although Aln and OPG could not prevent infection of necrotic bone adjacent to the implant, we found no evidence of biofilm formation anywhere else (Fig. 4A, B). In fact, we could readily identify active granulomas in immediate proximity to the pin that were completely Gram negative (Fig. 4C, D), indicating that anti-resorptive drugs do not interfere with innate immunity. In contrast, mice treated with TNFR:Fc had Gram positive biofilm in both necrotic bone and soft tissue adjacent to the pin (Fig. 4E–H). Furthermore, there was no evidence of an organized cellular immune response around the infected soft tissue (Fig. 4H). These results are consistent with the critical role for TNF in innate immunity and granuloma formation.

While considering alternative mechanisms responsible for the high-grade OM, we reflected on an explanation as to why the host chooses to mount such a vigorous osteolytic response to infection in which a much greater bone void is generated than what would be expected based on the margins of the biofilm (e.g. $>2mm^3$ vs. $<0.2mm^3$). The simplest explanation for this is that efficient drainage of the infection requires a large cavity for efflux of pus out of the medullary canal, which is under enormous intraosseous pressure from the recruitment and proliferation of immune cells and fluid. Thus, we reasoned that inhibition of cortical resorption would compromise this process as evidenced by a significant decrease in draining lymph node volume. To test this hypothesis we performed *in vivo* MRI to quantify the popliteal lymph node (PLN) volume on day 9 (data not shown), which demonstrated that both OPG, Aln and TNFR:Fc significant decrease PLN volume during the peak of infection. We also analyzed the tibiae and PLN of these mice *ex vivo*, which demonstrated two remarkable observations. First, there was no macroscopic evidence of pus draining from the pin tract of the OPG and Aln treated mice (Fig. 4I). This was to be expected based on the micro-CT data, which demonstrated the cortical hole is approximately the same size as the implant (Fig. 3). Secondly, OPG and Aln significantly inhibited the expansion of the draining PLN, but had no effects on the contralateral PLN, as determined by weight (Fig. 4J). Immunohistochemical analysis of these PLN with antibodies specific for B-cells (B220), T-cells (CD3), neutrophils (Neu7/4) and macrophages (F4/40) failed to generate any remarkable findings (data not shown), as the PBS samples simply appeared larger. We also performed flow cytometry to detect B220, CD4, CD8, CD11b, CD11c, and CD80 positive cells in PLN from infected and contralateral legs of mice treated with PBS or Aln (data not shown). The only significant finding was that Aln decreased the percentage of CD80+ cells (activated antigen presenting cells) by 20% versus PBS controls ($p < 0.02$). These results suggest that reduced lymphangiogenesis in the local draining lymph nodes after anti-resorptive therapy may be responsible for high-grade infections, but future studies are required to formally demonstrate the relationship between lymphatic egress from the infected medullary canal and PLN expansion during the establishment of OM.

DISCUSSION

Although infection rates following bone-implant surgery remain fairly low, the total number of OM cases is high[3], and the recent surge in MRSA further underscores the significance of this clinical problem[4]. At best, this catastrophic outcome requires a challenging revision surgery that is further complicated by deteriorated bone stock due to osteolysis. Thus, an important unanswered question regarding the treatment of patients with implant-associated OM is whether or not they would benefit from anti-resorptive therapy. Despite the successful case reports in the literature[5,6], our study indicates that this practice may be contraindicated since Aln and OPG: i) increase the amount of necrotic cortical bone around the implant that serves as a nidus for infection (Fig. 1), ii) significantly increases the incidence of high-grade

infections in mice during the establishment of OM (Fig. 2), and iii) reduce the cortical hole (Fig. 3) through which the opsonized bacteria and lymph must drain out of the wound (Fig. 4I, J).

Equally important to our positive findings are results that refute claims regarding the anti-angiogenic and immunosuppressive effects of anti-resorptive therapies. In search of the etiology of ONJ, others have reported that bisphosphonates inhibit capillary tube formation, vessel sprouting and circulating endothelial cells [14–16], and cited this as a mechanistic factor in the condition. In contrast, our vascular micro-CT analyses failed to demonstrate any drug effects on perfusable vessels >10μm (data not shown). Thus, our findings are more consistent with reports from others who have argued against this theory based on the fact that drugs such as thalidomide, with far greater anti-angiogenic capacity, do not result in ONJ [14]. Similarly, the findings that RANK signaling is required for lymph node development [32,33] and immunoregulatory co-stimulation [34,35] have led to a suspicion that RANK-ligand inhibition is immunosuppressive. However, our studies corroborate the prior findings of Stolina *et al*, who demonstrated that OPG treatment does not affect cell-mediated immune responses and granuloma formation [36], and the recent finding that humans genetically deficient in RANKL have severe osteopetrosis without immunodeficiency [37]. Therefore, we conclude that RANKL inhibition has insignificant immunoregulatory effects in the setting of *in vivo* pathogenic challenge, and that its ability to increase the incidence of high-grade OM can be entirely attributed to its effects on osteoclastic bone resorption, as these effects could be replicated with Aln (Figs. 1–3). To further abate concerns regarding the clinical use of a biologic RANKL inhibitor (i.e. denosumab [38]), we demonstrated that OPG and TNFR:Fc mediate similar effects on OM via different mechanisms, as evidenced by their differential effects on osteolysis, granuloma formation, and lymphatics. Given the remarkable clinical success of anti-TNF therapy over the last decade, and its much greater effects on the immune system compared to OPG, it is becoming more apparent that immunosuppression is unlikely to be a major limitation of biologic anti-resorptive therapy.

The most surprising results of our study was the observation that the massive bone void around the transtibial implant was largely due to inhibition of reactive bone formation rather than osteoclastic bone resorption, as evidenced by the micro-CT images of the Aln and OPG treated samples (Fig. 3A). Most interestingly is that this inhibition of bone formation appears as a perfectly symmetrical ring that extend >1mm from the biofilm adjacent to the pin. Thus, it is clear that this is mediated by an indirect mechanism that likely involves a secreted factor (i.e. noggin, DKK1, SOST) that has a gradient expression pattern originating from the infected bone. Elucidation of this factor(s) is now the subject of ongoing investigation, as it could also prove to be important for preventing inflammation mediated bone loss in aseptic conditions such as erosive arthritis and periprosthetic osteolysis.

While we do not want to overstate the implications of our findings as they relate to the emerging ONJ epidemic, we feel that there are several parallels that warrant discussion. The first and most frustrating is the absence of etiologic factors that are necessary and sufficient to faithfully reproduce OM and ONJ in similar individuals. Even though a correlation between ONJ and bisphosphonate use in cancer patients following oral surgery has been established, its overall incidence in this population is >10% [9,10]. Similarly, despite our best efforts in a controlled experiment model, we have been unable to establish conditions that lead to equivalent OM in genetically identical littermates, in which many of the mice that receive a Xen29 coated pin remain uninfected (Fig. 2). This indicates that stochastic epigenetic factors, such as the amount of necrotic bone available for bacterial adhesion, and the temporally restricted period for this event to occur, may be critical to the establishment of both OM and ONJ.

The other parallel that deserves mention is the potential association between inhibited lymphatics during the establishment of bone infection and bone pain. One potential mechanism by which anti-resorptive agents could inhibit lymphangiogenesis is by reducing the amount of VEGF-C produced during the infection through its effects on osteoclast precursors and osteoclasts, which produce high levels in response to RANKL[39]. Clinically, OM and ONJ are primarily discovered as a result of symptomatic bone pain, whose nature is largely unknown. Our novel finding that OPG and Aln drug inhibition of resorption is associated with significant decreased lymphatics during the establishment of bone infection implies that there must be a marked increase in intraosseous pressure at this time, which would be expected to induce bone pain characteristic of that seen in OM and ONJ. Interestingly, recent clinical studies have demonstrated that surgery-induced lymphedema is a major cause of local pain, and improvement of lymphatic drainage is an effective therapy in these patients [40]. Thus, the association of decreased lymph node size and drainage in our model of OM warrants further investigation.

Acknowledgments

This work was supported by research grants from the National Institutes of Health PHS awards AR48681, DE17096, AR52674, AR51469, AR46545, AR54041 and AR53459.

The authors would like to thank Dr. Christopher Beck of the Department of Biostatistics, for his assistance with the statistical analyses. We also thank Laura Yanoso for technical assistance with the micro-CT and Krista Scorsone for technical assistance with the histology. This work was supported by research grants for the US Dept. of Defense (ERMS No.06136016 and UID No. 99853) and the National Institutes of Health PHS awards AR48681, DE17096, AR52674, AR51469, AR46545, AR54041 and AR53459.

References

1. Lew DP, Waldvogel FA. Osteomyelitis. Lancet 2004;364–9431:369–79.
2. Toms AD, Davidson D, Masri BA, Duncan CP. The management of peri-prosthetic infection in total joint arthroplasty. J Bone Joint Surg Br 2006;88–2:149–55.
3. Darouiche RO. Treatment of infections associated with surgical implants. N Engl J Med 2004;350–14:1422–9.
4. Klevens RM, Morrison MA, Nadle J, Petit S, Gershman K, Ray S, Harrison LH, Lynfield R, Dumyati G, Townes JM, Craig AS, Zell ER, Fosheim GE, McDougal LK, Carey RB, Fridkin SK. Invasive methicillin-resistant Staphylococcus aureus infections in the United States. Jama 2007;298–15:1763–71.
5. Wright SA, Millar AM, Coward SM, Finch MB. Chronic diffuse sclerosing osteomyelitis treated with risedronate. J Rheumatol 2005;32–7:1376–8.
6. Soubrier M, Dubost JJ, Ristori JM, Sauvezie B, Bussiere JL. Pamidronate in the treatment of diffuse sclerosing osteomyelitis of the mandible. Oral Surg Oral Med Oral Pathol Oral Radiol Endod 2001;92–6:637–40.
7. Marx RE. Pamidronate (Aredia) and zoledronate (Zometa) induced avascular necrosis of the jaws: a growing epidemic. J Oral Maxillofac Surg 2003;61–9:1115–7.
8. Hellstein JW, Marek CL. Bisphosphonate osteochemonecrosis (bis-phossy jaw): is this phossy jaw of the 21st century? J Oral Maxillofac Surg 2005;63–5:682–9.
9. Shane E, Goldring S, Christakos S, Drezner M, Eisman J, Silverman S, Pendrys D. Osteonecrosis of the Jaw: More Research Needed. J Bone Miner Res 2006;21–10:1503–5.
10. Khosla S, Burr D, Cauley J, Dempster DW, Ebeling PR, Felsenberg D, Gagel RF, Gilsanz V, Guise T, Koka S, McCauley LK, McGowan J, McKee MD, Mohla S, Pendrys DG, Raisz LG, Ruggiero SL, Shafer DM, Shum L, Silverman SL, Van Poznak CH, Watts N, Woo SB, Shane E. Bisphosphonate-associated osteonecrosis of the jaw: report of a task force of the American Society for Bone and Mineral Research. J Bone Miner Res 2007;22–10:1479–91.
11. Hewitt C, Farah CS. Bisphosphonate-related osteonecrosis of the jaws: a comprehensive review. J Oral Pathol Med 2007;36–6:319–28.

12. Van den, Wyngaert T.; Huizing, MT.; Vermorken, JB. Osteonecrosis of the jaw related to the use of bisphosphonates. Curr Opin Oncol 2007;19–4:315–22.
13. Gutta R, Louis PJ. Bisphosphonates and osteonecrosis of the jaws: Science and rationale. Oral Surg Oral Med Oral Pathol Oral Radiol Endod. 2007
14. Marx RE, Sawatari Y, Fortin M, Broumand V. Bisphosphonate-induced exposed bone (osteonecrosis/osteopetrosis) of the jaws: risk factors, recognition, prevention, and treatment. J Oral Maxillofac Surg 2005;63–11:1567–75.
15. Ruggiero SL, Mehrotra B, Rosenberg TJ, Engroff SL. Osteonecrosis of the jaws associated with the use of bisphosphonates: a review of 63 cases. J Oral Maxillofac Surg 2004;62–5:527–34.
16. Allegra A, Oteri G, Nastro E, Alonci A, Bellomo G, Del Fabro V, Quartarone E, Alati C, De Ponte F, Cicciu D, Musolino C. Patients with bisphosphonates-associated osteonecrosis of the jaw have reduced circulating endothelial cells. Hematol Oncol. 2007
17. Bagan JV, Murillo J, Jimenez Y, Poveda R, Milian MA, Sanchis JM, Silvestre FJ, Scully C. Avascular jaw osteonecrosis in association with cancer chemotherapy: series of 10 cases. J Oral Pathol Med 2005;34–2:120–3.
18. Hansen T, Kunkel M, Weber A, James Kirkpatrick C. Osteonecrosis of the jaws in patients treated with bisphosphonates - histomorphologic analysis in comparison with infected osteoradionecrosis. J Oral Pathol Med 2006;35–3:155–60.
19. Li D, Gromov K, Soballe K, Puzas JE, O'Keefe RJ, Awad H, Drissi H, Schwarz EM. Quantitative mouse model of implant-associated osteomyelitis and the kinetics of microbial growth, osteolysis, and humoral immunity. J Orthop Res 2008;26–1:96–105.
20. Francis KP, Joh D, Bellinger-Kawahara C, Hawkinson MJ, Purchio TF, Contag PR. Monitoring bioluminescent Staphylococcus aureus infections in living mice using a novel luxABCDE construct. Infect Immun 2000;68–6:3594–600.
21. Rodan GA, Martin TJ. Therapeutic approaches to bone diseases. Science 2000;289–5484:1508–14.
22. Teitelbaum SL. Osteoclasts: what do they do and how do they do it? Am J Pathol 2007;170–2:427–35.
23. Zhang X, Xie C, Lin AS, Ito H, Awad H, Lieberman JR, Rubery PT, Schwarz EM, O'Keefe RJ, Guldberg RE. Periosteal progenitor cell fate in segmental cortical bone graft transplantations: implications for functional tissue engineering. J Bone Miner Res 2005;20–12:2124–37.
24. Hildebrand T, Laib A, Muller R, Dequeker J, Ruegsegger P. Direct three-dimensional morphometric analysis of human cancellous bone: microstructural data from spine, femur, iliac crest, and calcaneus. J Bone Miner Res 1999;14–7:1167–74.
25. Proulx ST, Kwok E, You Z, Papuga MO, Beck CA, Shealy DJ, Ritchlin CT, Awad HA, Boyce BF, Xing L, Schwarz EM. Longitudinal assessment of synovial, lymph node, and bone volumes in inflammatory arthritis in mice by in vivo magnetic resonance imaging and microfocal computed tomography. Arthritis Rheum 2007;56–12:4024–37.
26. Proulx ST, Kwok E, You Z, Beck CA, Shealy DJ, Ritchlin CT, Boyce BF, Xing L, Schwarz EM. MRI and quantification of draining lymph node function in inflammatory arthritis. Ann N Y Acad Sci 2007;1117:106–23. [PubMed: 17646265]
27. Ito H, Koefoed M, Tiyapatanaputi P, Gromov K, Goater JJ, Carmouche J, Zhang X, Rubery PT, Rabinowitz J, Samulski RJ, Nakamura T, Soballe K, O'Keefe RJ, Boyce BF, Schwarz EM. Remodeling of cortical bone allografts mediated by adherent rAAV-RANKL and VEGF gene therapy. Nat Med 2005;11–3:291–7.
28. Gortz B, Hayer S, Redlich K, Zwerina J, Tohidast-Akrad M, Tuerk B, Hartmann C, Kollias G, Steiner G, Smolen JS, Schett G. Arthritis induces lymphocytic bone marrow inflammation and endosteal bone formation. J Bone Miner Res 2004;19–6:990–8.
29. Schwarz EM, Benz EB, Lu AL, Goater JJ, Mollano AV, Rosier RN, Puzas JE, O'Keefe RJ. A Quantitative Small Animal Surrogate To Evaluate Drug Efficacy in Preventing Wear Debris-Induced Osteolysis. J Ortho Res 2000;18:849–55.
30. Li P, Schwarz EM, O'Keefe RJ, Ma L, Looney RJ, Ritchlin CT, Boyce BF, Xing L. Systemic tumor necrosis factor alpha mediates an increase in peripheral CD11bhigh osteoclast precursors in tumor necrosis factor alpha-transgenic mice. Arthritis Rheum 2004;50–1:265–76.

31. Flynn JL, Goldstein MM, Chan J, Triebold KJ, Pfeffer K, Lowenstein CJ, Schreiber R, Mak TW, Bloom BR. Tumor necrosis factor-alpha is required in the protective immune response against Mycobacterium tuberculosis in mice. Immunity 1995;2–6:561–72.
32. Dougall WC, Glaccum M, Charrier K, Rohrbach K, Brasel K, De Smedt T, Daro E, Smith J, Tometsko ME, Maliszewski CR, Armstrong A, Shen V, Bain S, Cosman D, Anderson D, Morrissey PJ, Peschon JJ, Schuh J. RANK is essential for osteoclast and lymph node development. Genes Dev 1999;13–18:2412–24.
33. Kong YY, Yoshida H, Sarosi I, Tan HL, Timms E, Capparelli C, Morony S, Oliveira-dos-Santos AJ, Van G, Itie A, Khoo W, Wakeham A, Dunstan CR, Lacey DL, Mak TW, Boyle WJ, Penninger JM. OPGL is a key regulator of osteoclastogenesis, lymphocyte development and lymph-node organogenesis. Nature 1999;397–6717:315–23.
34. Anderson DM, Maraskovsky E, Billingsley WL, Dougall WC, Tometsko ME, Roux ER, Teepe MC, DuBose RF, Cosman D, Galibert L. A homologue of the TNF receptor and its ligand enhance T-cell growth and dendritic-cell function. Nature 1997;390–6656:175–9.
35. Bachmann MF, Wong BR, Josien R, Steinman RM, Oxenius A, Choi Y. TRANCE, a tumor necrosis factor family member critical for CD40 ligand-independent T helper cell activation. J Exp Med 1999;189–7:1025–31.
36. Stolina M, Guo J, Faggioni R, Brown H, Senaldi G. Regulatory effects of osteoprotegerin on cellular and humoral immune responses. Clin Immunol 2003;109–3:347–54.
37. Sobacchi C, Frattini A, Guerrini MM, Abinun M, Pangrazio A, Susani L, Bredius R, Mancini G, Cant A, Bishop N, Grabowski P, Del Fattore A, Messina C, Errigo G, Coxon FP, Scott DI, Teti A, Rogers MJ, Vezzoni P, Villa A, Helfrich MH. Osteoclast-poor human osteopetrosis due to mutations in the gene encoding RANKL. Nat Genet 2007;39–8:960–2.
38. Schwarz EM, Ritchlin CT. Clinical development of anti-RANKL therapy. Arthritis Res Ther 2007;9 (Suppl 1):S7. [PubMed: 17634146]
39. Zhang Q, Guo R, Lu Y, Zhao L, Zhou Q, Schwarz EM, Huang J, Chen D, Jin ZG, Boyce BF, Xing L. VEGF-C, a Lymphatic Growth Factor, Is a RANKL Target Gene in Osteoclasts That Enhances Osteoclastic Bone Resorption through an Autocrine Mechanism. J Biol Chem 2008;283–19:13491–9.
40. Hamner JB, Fleming MD. Lymphedema therapy reduces the volume of edema and pain in patients with breast cancer. Ann Surg Oncol 2007;14–6:1904–8.

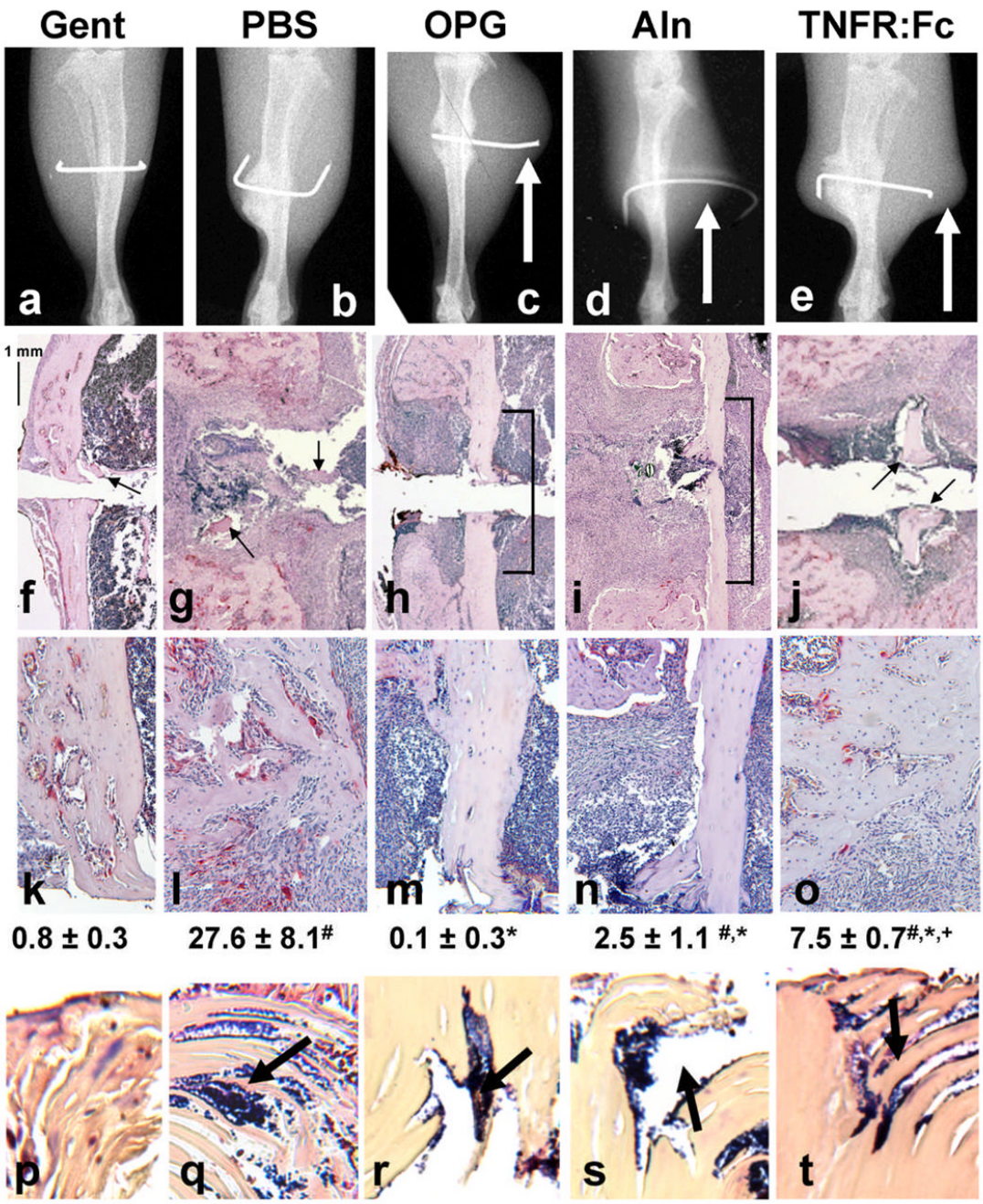

Figure 1. Anti-resorptive drugs increase the amount of necrotic bone around the infected implant during the establishment of OM

Mice (n=5) received a Xen29 infected transtibial pin and were treated with Gent, PBS, OPG, Aln and TNFR:Fc as indicated. Representative x-rays of the infected tibiae on day 18 are shown (**A–E**). Of note are the remarkable soft tissue abscesses around the pin in the OPG, Aln and TNFR:Fc treatment groups (arrows). Representative TRAP stained histology of the medial cortex of the infected tibiae are shown at 10x magnification (**F–J**) to demonstrate the remark differences in the amount of necrotic bone between the Gent, PBS and TNFR:Fc groups (arrows) and the OPG and Aln groups (brackets). These sections are also presented at 20x (**K–O**) to better illustrate differences in osteoclast numbers, which are presented as means ± SD

(# $p<0.05$ vs. Gent; * $p<0.05$ vs. PBS; + $p<0.05$ vs. OPG). Also of note is the large region of necrotic bone (void of osteocytes) adjacent to the live cortical bone in the OPG and Aln groups (**M–N**), while there is essentially no necrotic cortical bone adjacent to the infected pin in the other groups (**K, L, O**). Parallel sections were Gram stained and the necrotic bone fragments (arrows in **F, G, J**) or necrotic cortex (brackets in **H–I**) were photographed at 40x magnification (**P–T**) to demonstrate the absence or presence (arrows) of biofilm.

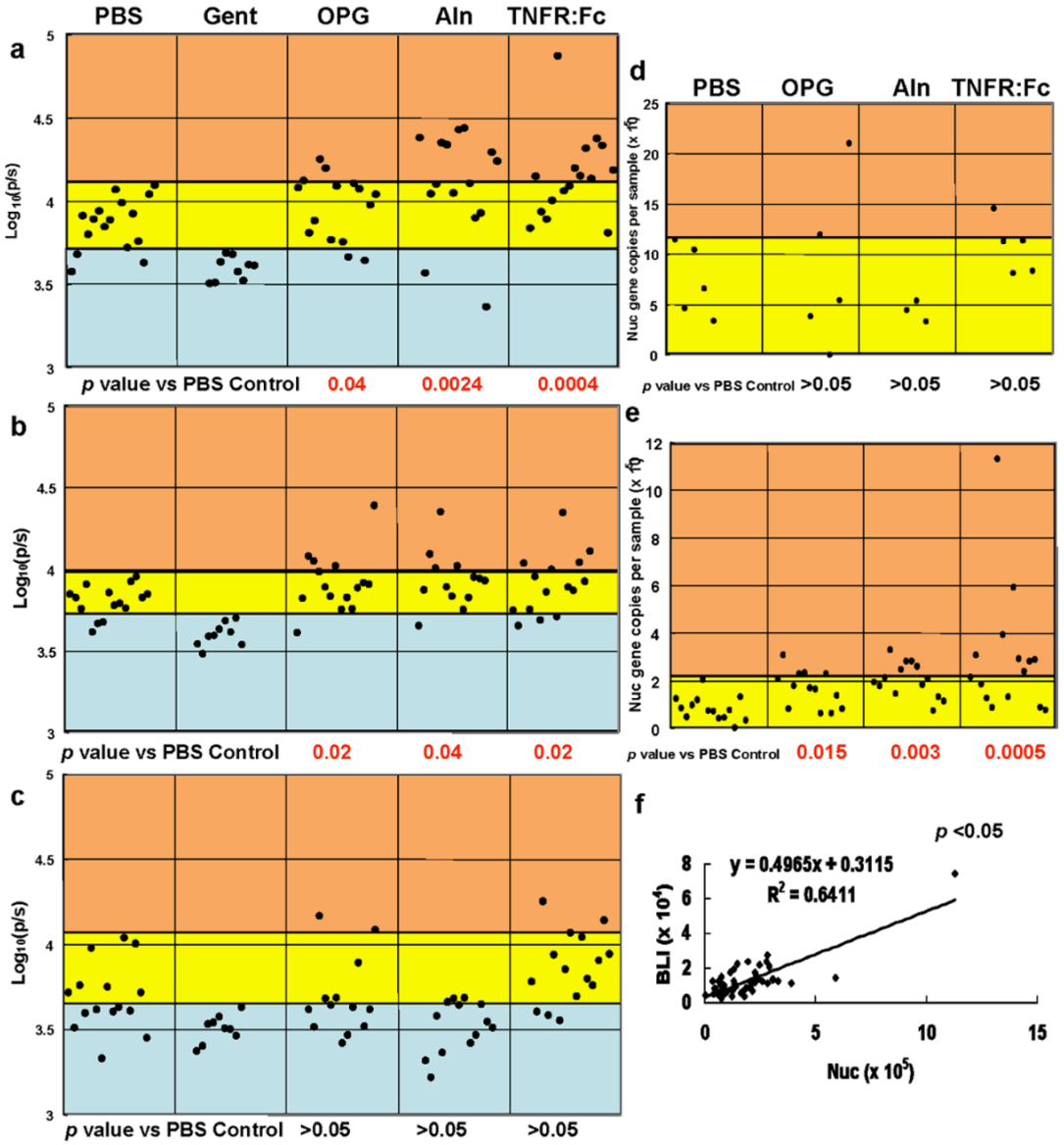

Figure 2. Anti-resorptive drugs increase the incidence of high-grade infections during the establishment of OM

Mice received a Xen29 infected transtibial pin and were treated with PBS (n=16), Gent (n=9), OPG (n=15), Aln (n=15) and TNFR:Fc (n=15) as indicated. The BLI signal of each mouse on day 7 (**A**), day 11 (**B**) and day 18 (**C**) post-infection is presented. To assess the drug effects on the incidence of "infections" and "high-grade infections", thresholds were defined by the greatest BLI value of the Gent group (blue region), and the greatest BLI value of the PBS group (yellow region) respectively. Thus, BLI values greater than the maximum threshold of the PBS group are regarded as high-grade infections (orange region). Mice were sacrificed on day 7 (D) or day 18 (E), and total DNA was extracted from the implanted tibia for *nuc*/*β-actin* RTQ-PCR as described in Methods. The data for each mouse is presented as the number of *nuc* genes per tibia standardized to a mouse *β-actin* control. The number of dots in each group corresponds to the number of animals in each group. Data for the Gent group are not included because *nuc* levels were undetectable. To assess the drug effects on bacterial load, a threshold was

defined by the greatest *nuc* gene value of the PBS group, which distinguishes infections (yellow region) from high-grade infections (orange region). A Fisher's exact test was performed to assess the significance of the high-grade infections. A linear regression analysis was performed with all of the day 18 data (n=56) to assess the relationship between BLI vs. *nuc* (**F**), and significance was determined using Pearson's correlation coefficient and a two-sided *t*-test.

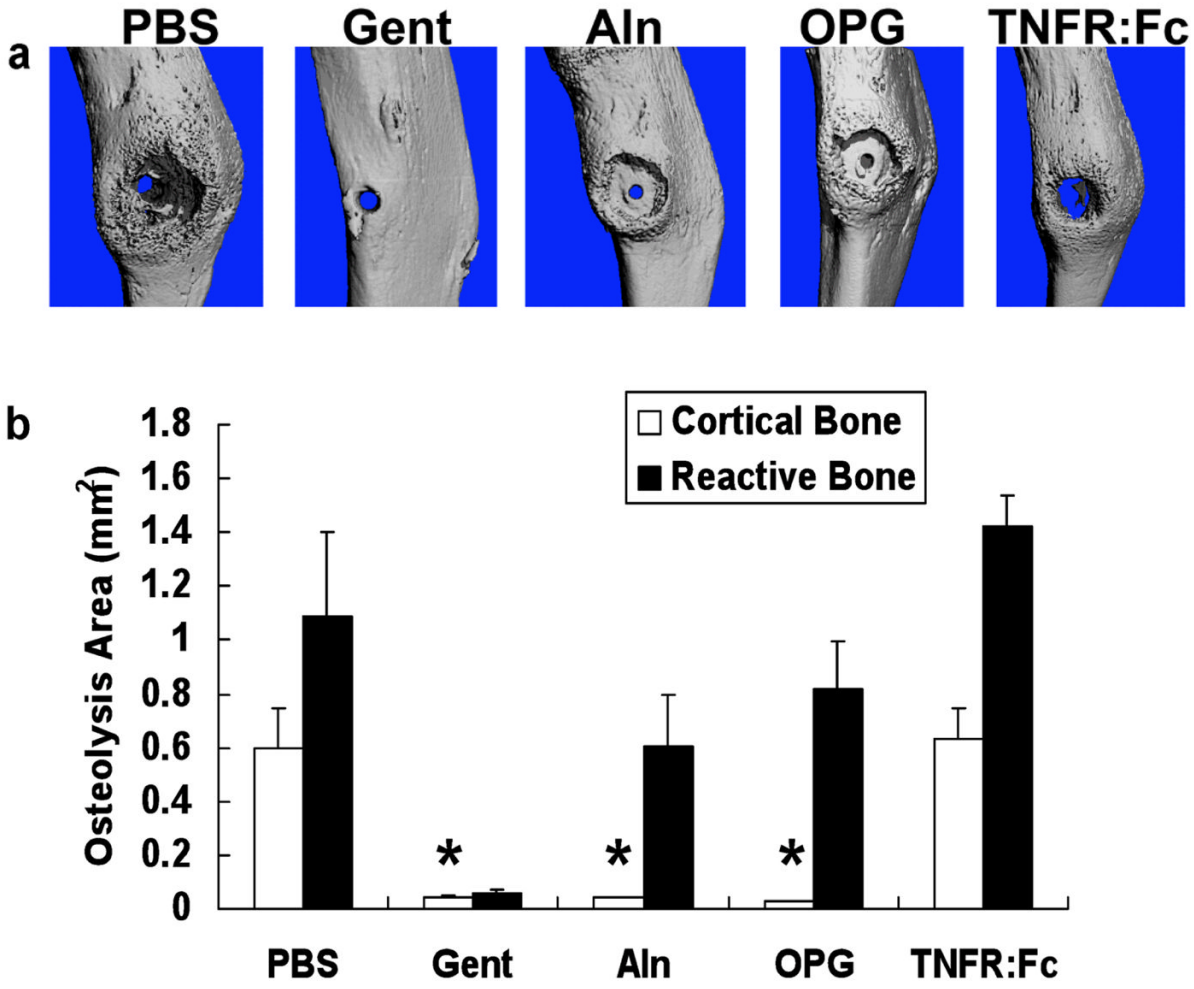

Figure 3. Anti-resorptive drug inhibition of cortical bone loss reveals that OM-induced osteolysis is due to osteoclastic activity and regional suppression of periosteal bone formation

Micro-CT scans of all of the tibiae described in Figure 1 were obtained before histology, and representative medial views of 3D reconstructed images from each group (n=5) are shown (A). Note the massive osteolysis in the PBS and TNFR:Fc controls, contrasted by its absence in the Gent control. Remarkably, both Aln and OPG prevented cortical bone loss, but did not prevent the OM inhibition of reactive bone formation around the infected pin, as evidence by the ~2mm diameter ring of exposed cortical bone centered on the pinhole. The maximum osteolysis area of the original cortex of the tibiae, and the area of the void of reactive bone around the implant were determined from 2D images as described in Methods (**B**). The data are presented as the mean ± SD (* $p < 0.05$ vs. PBS).

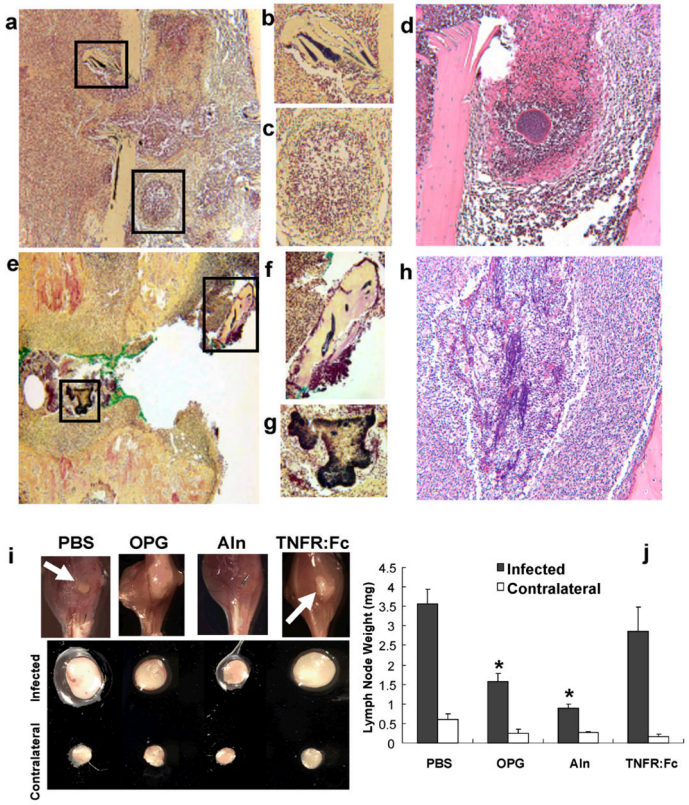

Figure 4. Anti-resorptive drugs inhibit draining lymph node expansion during the establishment of OM but are not immunosuppressive

Photographs of Gram stained histology of an infected mouse treated with Aln taken at 10x (A) and 20x (**B–C**) demonstrate that biofilms are only found in necrotic bone (**B**), and that granuloma form adjacent to the pin tract (**C**) in these animals. A photograph of a parallel section of the center of the granuloma stained with H&E is shown at 20x (**D**). Photographs of Gram stained histology of an infected mouse treated with TNFR:Fc taken at 10x (**E**) and 20x (**F–G**) demonstrate that biofilms are found in both necrotic bone (**F**), and the soft tissue adjacent to the pin tract (**G**) in these animals. No granulomas were found in any of the TNFR:Fc treated mice. A photograph of a parallel section of the soft tissue containing biofilm stained with H&E is shown at 20x (**H**). Mice (n=5) received a Xen29 infected transtibial pin and were given the indicated treatments as described in Figure 1. Photographs of representative infected legs from these mice 9 days post-surgery (**I**) demonstrate remarkable amounts of pus draining out of the tibiae of PBS and TNFR:Fc treated mice (arrows), which was not observed in the tibiae of OPG and Aln treated animals. The PLN from the infected and contralateral leg of these mice are also shown to demonstrate their remarkable differences in size. The PLN from all of the mice were weighed to quantify the differences in size (J), and the data are presented as the mean ± SD (* $p < 0.05$ vs. PBS).